*International Journal on Emerging Technologies* **15**(1): 09-15(2024)

**ISSN No. (Print): 0975-8364**
**ISSN No. (Online): 2249-3255**

# Transient Laminar Film Condensation on an Isothermal Vertical Surface in an Anisotropic Permeability Porous Medium using the Complementary Error Function for the Temperature Profile

***S.A.O. Sanya[1*], G. Chidikofan[1], M.F.O. Sanya[2], S. Osseni[1] and C. Akowanou[1]***
*[1]Applied Mathematical and Engineering Science Laboratory (LSIMA), Benin Republic, BP : 2282 Goho Abomey,*
*[2]Applied Mechanical and Engineering Laboratory - Polytechnic School of Abomey-Calavi, University of Abomey-Calavi, Benin Republic, 01 B.P. 2009, Cotonou*

*(Corresponding author: S.A.O. Sanya*)*
*(Received 25 November 2023, Revised 15 January 2023, Accepted 02 February 2024)*
*(Published by Research Trend, Website: www.researchtrend.net)*

**ABSTRACT: This paper concerns the transient liquid film condensation phenomenon on an isothermal vertical surface in contact with an anisotropic porous medium using the complementary error function for the temperature profile. The boundary layer equations are formulated and the time variable is involved only in the energy equation. The governing equations of the problem have been solved analytically by the similarity method using the Kärman-Pholhausen integral method. Thus, the expressions of the dimensionless thickness of the liquid film, the Nusselt number and the characteristic limit time of the transition from transient to steady state have been developed. The results found allows to extend the isotropic porous medium to take into account the anisotropic properties of the porous medium, using the flow permeability tensor and the generalised Darcy's law to describe the fluid flow in the porous medium. A good remark has been done for the temperature profile which is assumed as the complementary error function and gives the same results as the previous studies using a linear function.**

**Keywords:** Transient film condensation, complementary error function, anisotropic porous medium, Darcy flow model.

## INTRODUCTION

Liquid Film condensation heat transfer is a common phenomenon in industrial processes such as refrigerating machines and heat pumps, steam heating systems, heat exchangers and distillation systems in seawater desalination plants (Sanya *et al.*, 2014; Degan *et al.*, 2016). The first work began by Nusselt (1916) who considered pure saturated steam in contact with a vertical flat wall. The condensation heat transfer problem has continued to attract considerable attention (Mendez and Trevino, 1997; Chen *et al.*, 1987). Cheng (1981) established similarity solutions for steady filmwise condensation in a constant-porosity medium. In his study, he investigated laminar filmwise condensation along a wedge and showed that a linear temperature profile was a reasonable assumption for small values of Jakob number (i.e. Ja < 1). But his results overestimated the effects of condensation heat transfer. Most of the work has often focused on Darcy's model, which assumes a proportionality between fluid velocity and pressure gradient to describe fluid flow in the porous medium (Liu *et al.*, 1984).

There is also increasing interest in work under transient conditions. Cheng and Chui (1984b) considered the problem of transient liquid film condensation on a vertical surface in an isotropic porous medium. They used the Kärman-Pholhausen integral method and the similarity method to deduce the liquid film thickness and the local Nusselt number.

The objective of present study is to deduce the influence of the permeability anisotropy parameters of the porous medium on the thickness of the liquid film on the vertical surface studied, as well as on the heat transfer flow at the surface, for a transient regime using the complementary error function for the temperature profile. The Darcy model is generalised by taking into account the permeability anisotropy tensor (Degan *et al.*, 1995). It is employed to describe the characteristics of the liquid saturated region in the anisotropic porous medium which the complementary error function is used for the temperature profile. Then, the analytical results are obtained for the dimensionless liquid film thickness, the Nusselt number and the characteristic limit time.

## METHODS

### *A. Mathematical formulation*

On the Fig. 1, the physical model adopted is a vertical plate of low thickness, height $L$ and inner surface temperature $T_w$, which is in direct contact with the porous medium with anisotropic permeability. The coordinate axes $(Ox)$ and $(Oy)$ are aligned respectively with the vertical and horizontal directions. The permeability along the two principal axes of the porous matrix are denoted by $K_1$ and $K_2$. The permeability anisotropy of the porous medium is characterised by the permeability ratio $K^* = K_1/K_2$ and the orientation angle $\varphi$ defined between the horizontal direction and the main permeability axis $K_2$. Inside this porous medium flows a pure saturated vapour with a saturation temperature $T_S$ higher than the surface temperature $T_w$. As the vapour flows through the porous medium, condensation of the vapour occurs on the wall leading to the formation of a thin liquid film with a thickness $\delta_L$along the vertical surface. As a result, there are two areas: the porous medium saturated by the liquid film dropping on the wall and the saturated vapour in the rest of the porous space with anisotropic permeability. In addition, the following assumptions are assumed as those of Cheng (1981), namely that the liquid-vapour interface is quite distinct, the properties of the porous medium are such that those of the liquid film and vapour are constant, the boundary layer approximations are applicable to the phenomenon near to the vertical surface and the time variable is involved only in the energy equation as those of Cheng and Chui (1984b). Generalised Darcy's law is also used to describe the fluid flow in the porous medium and then the momentum equations can be deduced.

Thus, the governing equations of the problem, in compact form, are deduced, namely the following continuity (1), momentum (2) and energy (3) equations:

$$\frac{\partial\rho}{\partial t} + \vec{\nabla}.\left(\rho\vec{V}\right) = 0 \qquad (1)$$

$$\vec{V} = \frac{\bar{\bar{K}}}{\mu}\left(-\vec{\nabla}P + \rho\vec{g}\right) \qquad (2)$$

$$\frac{\partial T}{\partial t} + \vec{V}.\vec{\nabla}T = \alpha_c\nabla^2 T \qquad (3)$$

Where, $P$ is the pressure in the porous medium, $\rho$ the density of the fluid, $\vec{g}$ the gravitational acceleration vector, $\mu$ the dynamic viscosity of the fluid, $\vec{V}$ the velocity vector of the fluid in the porous medium, $\alpha$ is the thermal diffusivity of the fluid and $\left(\bar{\bar{K}}\right)^{-1}$the inverse symmetrical second-order permeability tensor defined in the cartesian coordinates as (Degan *et al.* (1995):

$\left(\bar{\bar{K}}\right)^{-1} = \frac{1}{K_1}\begin{bmatrix} a & -c \\ -c & b \end{bmatrix}$ with $a = cos^2\varphi + K^* sin^2\varphi$, $b = K^* cos^2\varphi + sin^2\varphi$ and $c = \frac{1}{2}(1 - K^*)\sin 2\varphi$.

The writing of equations (1), (2) and (3) in the region of the liquid film become in primitive form:

$$\frac{\partial u_L}{\partial x} + \frac{\partial v_L}{\partial y} = 0 \qquad (4)$$

$$u_L = \frac{K_1}{a\mu_L} g(\rho_L - \rho_v) \qquad (5)$$

$$\frac{\partial T}{\partial t} + u_L\frac{\partial T}{\partial x} + v_L\frac{\partial T}{\partial y} = \alpha_c\frac{\partial^2 T}{\partial y^2} \qquad (6)$$

Where the equation (5) is obtained from the previous study by Degan *et al*. (2016) under the aforementioned assumptions and the ratio of the heat capacities and the thermal diffusivity of the liquid in porous medium are defined as follows:

$$\sigma = \frac{(\rho c_P)_c}{(\rho c_P)_L} \qquad (7)$$

$$\alpha_c = \frac{k_c}{(\rho c_P)_L} \qquad (8)$$

Where $(\rho c_P)_c$ and $k_c$ are the heat capacity and the thermal conductivity of the fluid-filled porous medium defined by Cheng and Chui (1984b) as $(\rho c_P)_c = (1 - \emptyset)(\rho c_P)_p + \emptyset(\rho c_P)_L$ and $k_c = (1 - \emptyset)k_p + \emptyset k_L$ where $\emptyset$ is the porosity and the subscripts « p » and « L » denote the quantities associated respectivily with the porous medium and the saturated liquid.

In addition, the initial and boundary conditions associated with the preceding governing equations are as follows:

- ❖ Initial condition: $T(x, y, 0) = T_S$ (at $t = 0$) (9)
- ❖ Boundary condition at the vertical surface: $T(x, 0, t) = T_W, \quad t > 0$ (10)
- ❖ Boundary condition at liquid-vapour interface: $T(x, \delta_L, t) = T_S$ (11)

*B. Scale analysis*

Based on the work of Bejan (1984) and designating as $L$ and $\delta_L$ respectively the orders of magnitude on the $x$ and $y$ axes, in the liquid boundary layer region where $\delta_L \ll L$, equations (4), (5) and (6) obey the following orders of magnitude:

$$\frac{u_L}{L} \sim \frac{v_L}{\delta_L} \qquad (12)$$

$$u_L \sim \frac{K_1}{\mu_L} g(\rho_L - \rho_v) \qquad (13)$$

$$\left(\sigma\frac{\Delta T}{t}\delta_L\right), \left(u_L\frac{\Delta T}{LRa_L}\delta_L\right), (v_L\Delta T) \sim \left(\frac{h_{fg}}{c_{pL}}\frac{u_L}{LRa_L}\delta_L\right), \left(\frac{h_{fg}}{c_{pL}}\frac{\delta_L}{t}\right), \left(\alpha_c\frac{\Delta T}{\delta_L}\right) \qquad (14)$$

In equation (14), $\Delta T$is such that :

$$\Delta T = (T_W - T_S) \qquad (15)$$

Considering the orders of magnitude of equations (12) to (14), the following results are obtained for $\delta_L, u_L, v_L$ and $t$ :

$$\delta_L \sim L \qquad (16)$$

$$u_L \sim \frac{\alpha_c}{L} Ra_L \qquad (17)$$

$$v_L \sim \frac{\alpha_c}{L} \qquad (18)$$

$$t \sim \frac{\sigma L^2}{\alpha_c} \qquad (19)$$

The Rayleigh number is defined in equation (17):

$$Ra_L = \frac{K_1 g L}{\mu_L \alpha_c}(\rho_L - \rho_V) \qquad (20)$$

*C. Resolution*

Taking into account the orders of magnitude $LRa_L$, $L$, $\alpha_c Ra_L/L$, $\alpha_c/L$, $\Delta T$, $\sigma L^2/\alpha_c$ respectively for the $x$ and y axes, the $x$ and y components of velocity, temperature and time, the governing equations (4), (5) and (8) take the following dimensionless form:

$$\frac{\partial U_L}{\partial X} + \frac{\partial V_L}{\partial Y} = 0 \qquad (21)$$

$$U_L = \frac{1}{a} \qquad (22)$$

$$\int_0^A \frac{\partial\theta_L}{\partial\tau} dY + \frac{1}{a}\int_0^A \frac{\partial\theta_L}{\partial X} dY = \left(\frac{\partial\theta_L}{\partial Y}\right)_{Y=A} - \left(\frac{\partial\theta_L}{\partial Y}\right)_{Y=0} \qquad (23)$$

Where $A$ is the dimensionless thickness of the liquid film defined as:

$$A = \frac{\delta_L}{L} \tag{24}$$

$$\left(\frac{\partial \theta_L}{\partial Y}\right)_{Y=A} = -\frac{1}{a\,Ja}\frac{\partial A}{\partial X} - \frac{1}{\sigma Ja}\frac{\partial A}{\partial \tau} \tag{25}$$

Equation (23) can be solved under the following dimensionless boundary conditions:

$$\tau = 0, \quad \theta_L(X, Y, 0) = 0 \tag{26a}$$

$$Y = 0, \quad \theta_L(X, 0, \tau) = 1 \tag{26b}$$

$$Y = A, \quad \theta_L(X, A, \tau) = 0 \tag{26c}$$

We consider the following temperature profile that satisfies the boundary condition (26b), defined by Cheng and Pop (1984a) as:

$$\theta_L(\eta) = erfc(\eta) \tag{27}$$

Where $erfc$ is the complementary error function and $\eta$ represents the variable defined as follows:

$$\eta = \frac{Y}{A} \tag{28}$$

Substituting equations (27) and (28) in equation (23), the following equation is obtained:

$$\left[\xi + \frac{1}{\sigma Ja}\right]\frac{\partial A}{\partial \tau} + \frac{1}{a}\left[\xi + \frac{1}{Ja}\right]\frac{\partial A}{\partial X} = \frac{2}{A\sqrt{\pi}} \tag{29}$$

$\xi$is the parameter such that:

$$\xi = \int_0^1 \theta_L(\eta)\, d\eta \tag{30}$$

Equation (29) can be solved under the following dimensionless boundary conditions:

$$\tau = 0, \quad A(X, 0) = 0 \tag{31a}$$

$$\tau \geq 0, \quad A(0, \tau) = 1 \tag{31b}$$

Equation (29) is a partial differential equation of the hyperbolic type which will be solved by the method of characteristics through the following system of differential equations:

$$\frac{2}{\left[\xi + \frac{1}{\sigma Ja}\right]} d\tau = A dA = \frac{2a}{\left[\xi + \frac{1}{Ja}\right]} dX \tag{32}$$

Equation (32) has the following characteristic:

$$dX = \frac{\left[\xi + \frac{1}{Ja}\right]}{\left[\xi + \frac{1}{\sigma Ja}\right]} d\tau \tag{33}$$

Parameter $A$can then be deduced from the following relationships:

❖ For transient film condensation:

$$\left[\xi + \frac{1}{\sigma Ja}\right] A dA = 2\mathrm{d}\tau \tag{34}$$

❖ For steady film condensation:

$$\left[\xi + \frac{1}{Ja}\right] A dA = 2a dX \tag{35}$$

By integrating equation (34) with condition (31a), the equation (36) is obtained in the case of transient regime:

$$A = \left\{\sqrt{\pi}\left(\xi + \frac{1}{\sigma Ja}\right)\right\}^{-1/2} \tau^{1/2} \tag{36}$$

Similarly, by solving equation (35) subject to condition (31b), expression (37) is found in steady state:

$$A = 2a^{\frac{1}{2}}\left\{\sqrt{\pi}\left(\xi + \frac{1}{Ja}\right)\right\}^{-\frac{1}{2}} X^{\frac{1}{2}} \tag{37}$$

Thus, the expression of $A$ changes according to equations (36) and (37) along the boundary characteristic line:

$$\tau_C = a\frac{\left[\xi + \frac{1}{\sigma Ja}\right]}{\left[\xi + \frac{1}{Ja}\right]} X \tag{38}$$

Equation (38) shows the limit time for the regime to move from the transient case to steady state case. The corresponding temperature profile can now be deduced.

❖ In the case where $\tau < \tau_C$, the expression (39a) is found :

$$\theta_L(\eta) = erfc\left\{\frac{y}{2}\left\{\sqrt{\pi}\left(\xi + \frac{1}{\sigma Ja}\right)\right\}^{1/2} \tau^{-1/2}\right\} \tag{39}$$

❖ In the case where $\tau > \tau_C$, the expression (39b) is found:

$$\theta_L(\eta) = erfc\left\{\frac{y}{2} a^{-1/2}\left\{\sqrt{\pi}\left(\xi + \frac{1}{Ja}\right)\right\}^{1/2} X^{-1/2}\right\} \tag{40}$$

Using equations (27), (28), (37) et (39), the expression of the heat flux for the transient case can be deduced where $\tau < \tau_C$:

$$q_w = \frac{k(T_W - T_S)}{\sqrt{\pi}}\left\{\sqrt{\pi}\left(\xi + \frac{1}{\sigma Ja}\right)\right\}^{1/2}\left(\frac{\sigma}{\alpha_C t}\right)^{1/2} \tag{41}$$

The local Nusselt number is given by the formula (42):

$$Nu_x = \frac{q_w\, x}{k(T_W - T_S)} \tag{42}$$

In other words, in the region $\tau < \tau_C$, the local Nusselt number is as follows:

$$\frac{Nu_x}{\sqrt{Ra_{x,L}}} = \left\{\frac{\left(\xi + \frac{1}{\sigma Ja}\right)}{\sqrt{\pi}}\right\}^{\frac{1}{2}}\left(\frac{\tau}{X}\right)^{-\frac{1}{2}} \tag{43}$$

Similarly, considering equations (29), (30), (31a) and (40), the expression of the heat flow for the steady state case can be obtained where $\tau > \tau_C$:

$$q_w = \frac{k(T_W - T_S)}{x}\left\{\frac{\left(\xi + \frac{1}{Ja}\right)}{a\sqrt{\pi}} Ra_{x,L}\right\}^{1/2} \tag{44}$$

The expression (45) can be deduced from this:

$$\frac{Nu_x}{\sqrt{Ra_{x,L}}} = \left\{\frac{\xi + \frac{1}{Ja}}{a\sqrt{\pi}}\right\}^{1/2} \tag{45}$$

## RESULTS AND DISCUSSION

Fig. 2 shows the variations of the limit time $\tau_C$ at the end of which the steady state is reached, when the plate is subjected to condensation phenomena by natural convection. It can be seen from this figure that $\tau_C$varies linearly as a function of the distance $X$ counted on the surface from the leading edge when the Jakob number is equal to2.0 and $\sigma$ =0.6, for an orientation angle of the main axes of permeability $\varphi = 30°$and for different values of the anisotropy ratio $K^*$. This line is also justified by considering equation (38) and divides the plane $(X, \tau)$ into two half planes for which a different flow mode corresponds respectively. The lower half plane defined for times $\tau$ $(\tau < \tau_C)$ is the seat of pure conduction through the porous medium, while the upper half-plane is the region dominated by convective heat transfer at times $\tau(\tau > \tau_C)$, according to the work carried out by Degan *et al.* (2007). Moreover, for a given distance $X$, when the anisotropy ratio decreases, the decrease in the time $\tau_C$ taking by the condensation phenomena to pass from the transient regime to the steady state is noticed. This implies in the plane $(X, \tau)$ to an extension of the domain corresponding to the upper half plane delimited by $\tau_C$.

Fig. 3 illustrates the variation of the dimensionless time $\tau_C$ as a function of the distance $X$, expressed by equation (42), for different values of the angle $\varphi$, when $K^* = 2.5$, $Ja = 2.0$ and $\sigma$ =0.6. The same remark as the previous work (Sanya *et al.*, 2021) can be concluded that the time $\tau_C$ at which the steady state is reached increases as a function of the increase of the orientation angle $\varphi$ of the main axes of the anisotropic permeability porous medium. This increase of the limit dimensionless time $\tau_C$ reflects the persistence of the transient regime before the appearance of the permanent regime.

Fig. 4 illustrates the effect of the time on the dimensionless thickness $A$of the liquid film along a vertical surface for various values of Jakob number for $\sigma = 0.6$. It can be noticed that the dimensionless thickness of the liquid film increases continuously with time but it decreases for the increase value of the Jakob number, in the transient state. This trend follows from the fact that the dimensionless thickness of the liquid film is proportional to $\tau^{1/2}$ (Eq. (36)) and inversely proportional to $Ja^{1/2}$, such that increasing Jakob number implies the diminution of the dimensionless thickness of the liquid film which becomes less and less affected by time. The same behavior is observed in Figure 5 illustrating the effect of the time on the dimensionless thickness of the liquid film along a vertical surface for various values of heat capacity ratio $\sigma$ for $Ja = 10.0$. The dimensionless thickness $A$ drops progressively as $\sigma$ is made weaker, independently of the time $\tau$, but this decreasing is less drastic than it can be observed in Fig. 4.

Fig. 6 shows the variation of the heat transfer rate $Nu_x/(Ra_{x,L})^{1/2}$ for different values of the ratio of the anisotropy permeability coefficients and for $\varphi = 30°$, $Ja = 2.5$ and $\sigma = 0.6$. With regard to the general trend, it can be seen that the heat transfer rate decreases over time, corresponding to the transient period $(\tau < \tau_C)$, and ends up maintaining a constant value from the limit time $\tau_C$at which the steady state begins$(\tau > \tau_C)$. During this steady state, where the time variable no longer has any influence, the heat transfer rate decreases as the ratio of the anisotropic permeability coefficients increases. The same decrease is also observed in Figure 7 for an increase in the orientation angles of anisotropic permeability of the porous medium. Moreover, in the transient regime, anisotropic permeability of the porous medium has no influence. A good remark can be made when $K^* = 1.0$ in Fig. 6 or $\varphi = 0$ in Fig. 7 which implies that $a = 1$ and the result is similar to that obtained analytically by Cheng and Chui (1984b) for the isotropic porous medium. This behavior can also be proved from the fact that, according to equation (5), when the parameters $K^*$ and $\varphi$ are held constant respectively to 1.0 (that is to say $K_1 = K_2 = K$) and 0, the velocity of the liquid film in the anisotropic porous medium $u_L$ is the same to that found by Cheng and Chui (1984b) in the case of isotropic porous medium.

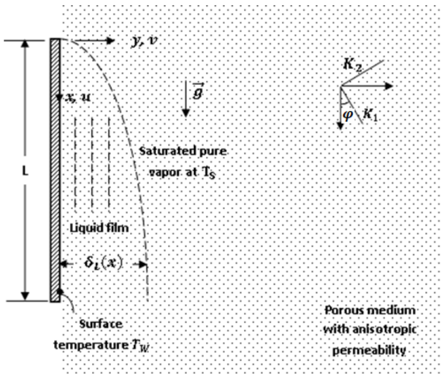


**Fig. 1.** Physical situation and coordinate system.

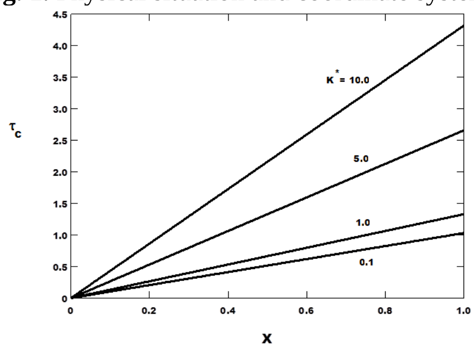


**Fig. 2.** Effect of the ratio of anisotropic permeability coefficients on the characteristic limit time $\tau_C$ for $\varphi = 30°$, $Ja = 2.0$ and $\sigma = 0.6$.

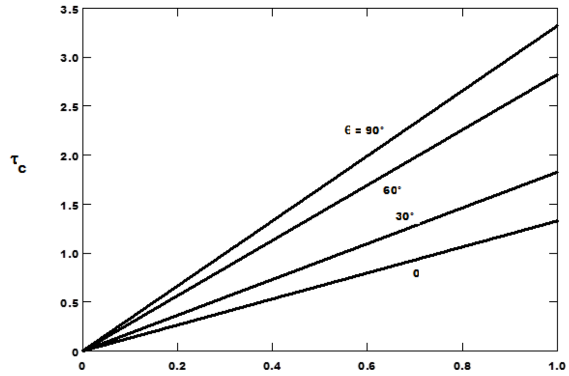


**Fig. 3.** Effect of the orientation angle of the main axes on the characteristic limit time $\tau_C$ for $K^* = 2.5$, $Ja = 2.0$ and $\sigma = 0.6$.

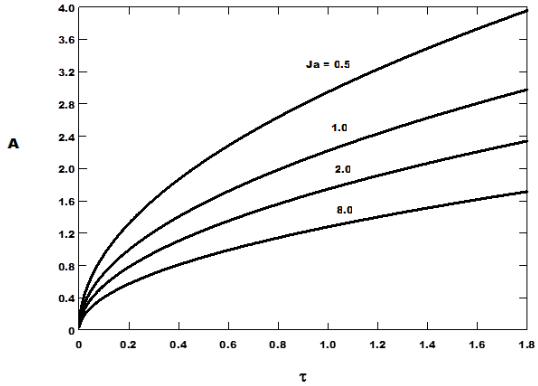


**Fig. 4.** Effect of the time on the dimensionless thickness of the liquid film for various values of Jakob number for $\sigma = 0.6$.

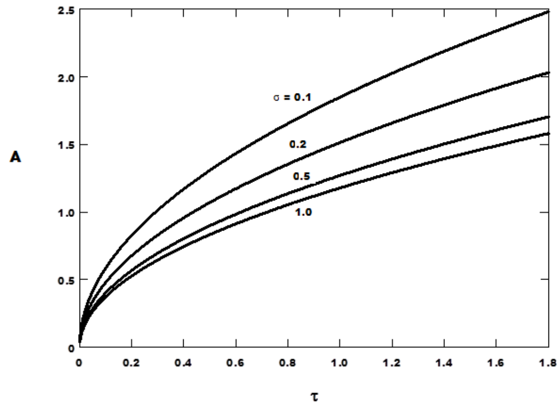


**Fig. 5.** Effect of the time on the dimensionless thickness of the liquid film for various values of heat capacity ratio σ for $Ja = 10.0$.

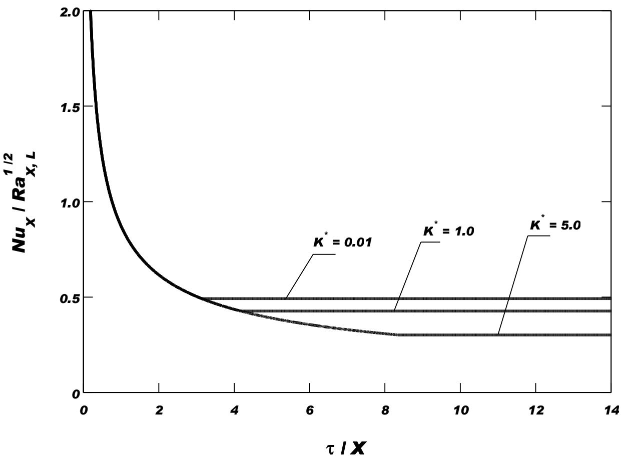


**Fig. 6.** Effect of the ratio of the anisotropic permeability coefficients on the heat transfer rate $Nu_x/Ra_{x,L}^{1/2}$ for $\varphi = 30°$, $Ja = 2.5$ and $\sigma = 0.6$.

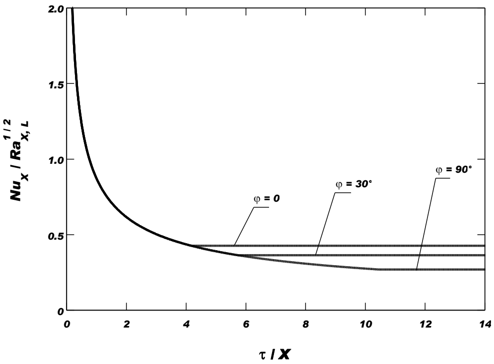


**Fig. 7.** Effect of the orientation angle of the main axes on the heat transfer rate $Nu_x/Ra_{x,L}^{1/2}$ for $K^* = 3.0$, $Ja = 2.5$ and $\sigma = 0.6$.

**Nomenclature**

| | |
|---|---|
| $a, b, c$ | Anisotropy constants in permeability |
| A | Dimensionless film thickness, $\delta_L/L$ |
| $c_P$ | Specific heat capacity of fluid at constant pressure $(J.kg^{-1}.K^{-1})$ |
| $g$ | Gravitational acceleration $(m.s^{-2})$ |
| $h$ | Latent heat of condensation $(J.kg^{-1})$ |
| $Ja$ | Jakob number, $Ja = \frac{Cp_L(T_S-T_W)}{h_{Lv}}$ |
| $\bar{\bar{K}}$ | Flow permeability anisotropic tensor |
| $K_1, K_2$ | Flow permeability along the principal axes $x, y$ respectivily $(m^2)$ |
| $K^*$ | Anisotropic permeability ratio, $K_1/K_2$ |
| $k_L$ | Effective thermal conductivity of the liquid film in porous medium $(W.m^{-1}.K^{-1})$ |
| $L$ | Height of the verticale surface $(m)$ |
| $Nu_x$ | Local Nusselt number |
| $P$ | Pressure $(Pa)$ |
| $q$ | Local heat transfer rate transmitted to the condensing surface |
| $Ra_L$ | Rayleigh number, $Ra_L = \frac{K_1 gL}{\mu_L \alpha_L}(\rho_L - \rho_v)$ |
| $Ra_{x,L}$ | Local Rayleigh number |
| $T$ | Temperature $(K)$ |
| $t$ | Time (s) |
| $\tau$ | Dimensionless time |
| $\tau_C$ | Dimensionless time of the changing flow mode from transient to steady state |
| V | Velocity of the liquid film in the porous medium $(m.s^{-1})$ |
| $u_L, v_L$ | Velocity components in $x, y$ directions $(m.s^{-1})$ |
| $x, y$ | Cartesian coordinates $(m)$ |

**Greek symbols**

| | |
|---|---|
| $\alpha_c$ | Thermal diffusivity of the fluid-filled porous medium $(m^2.s^{-1})$ |
| $\delta_L$ | Liquid film thickness $(m)$ |
| $\eta$ | Similarity variable |
| $\mu$ | Dynamic viscosity of the fluid $(kg.m^{-1}.s^{-1})$ |
| $\lambda$ | Parameter defined in equations (38) and (41) |
| $\theta_L$ | Dimensionless temperature profile in the liquid film, $(T_L - T_S)/\Delta T_L$ |
| $\rho$ | Density of the fluid $(kg.m^{-3})$ |
| $\sigma$ | Heat capacity ratio, $\sigma = (\rho c_p)_c/(\rho c_p)_L$ |
| φ | Orientation angle of main axes (°) |

**Superscript**

| | |
|---|---|
| $*$ | Dimensional quantities |

**Subscripts**

| | |
|---|---|
| $p$ | refers to porous medium |
| $L$ | refers to liquid region |
| $s$ | refers to saturation condition |
| $w$ | refers to the vertical surface |

## CONCLUSIONS

This study copes with liquid film condensation along a vertical surface embedded in anisotropic porous medium whose principal axes are non-coincident with the gravity vector. With the formulation of the problem on the basis of the generalized Darcy's law, boundary-layer equations are solved analytically by the method of characteristics, as time is taken into account in equation of energy. By the end, the results obtained for the temperature profile assuming as a complementary error function have the same trends with those for the temperature profile assuming as linear function (Sanya *et al*., 2021):

1. The transient convective flow along a vertical plate has a singularity characterised by the transition that the convective flow undergoes from a regime where instabilities movements in the porous medium prevail to a regime characterised by stationary movements which take place from a limit dimensionless time $\tau_C$ counted from the initial moment of heating of the surface by the initiation of the condensation phenomena. This time $\tau_C$ corresponds to the time from which the characteristic quantities of heat and mass transfer suddenly change from the transient one-dimensional conduction regime to a two-dimensional natural convection regime near to the vertical surface where a steady-state regime now prevails. The limiting dimensionless time $\tau_C$ to reach the steady state increases with increasing the anisotropy ratio $K^*$ and the orientation angle $\varphi$ of the main axes of the porous medium.
2. The dimensionless thickness of the liquid boundary layer shows the same pattern as that obtained for the case of isotropic porous medium in the transient regime by previous work.
3. The heat transfer rate depends on the time variable in the transient regime and the anisotropy permeability parameters in the steady state.

**Acknowledgement.** Thanks to all who give their valuable suggestions and comments to this paper.

## REFERENCES

Chen, S. L., Gerner, F. M. and Tien, C. L. (1987). Film condensation correlations. *Experimental Heat Transfer, 1*, 93-107.

Cheng, P. and Pop, I. (1984a). Transient free convection about a vertical flat plate embedded in a porous media. *Int. J. Eng. Sci, 22*, 253-264.

Cheng, P. (1981). Film condensation along an inclined surface in porous medium. *Int. J. Heat Mass Transfer*, *24*, 983-990.

Cheng, P. and Chui, D. K. (1984b). Transient film condensation on a vertical surface in a porous medium. *Int. J. Heat Mass Transfer*, *27*, 795-798.

Degan, G., Vasseur, P. and Bilgen, E. (1995). Convective heat transfer in a vertical anisotropic porous layer.*Int. J. Heat Mass Transfer*, *38*(11), 1975-1985.

Degan, G., Sanya, A. and Akowanou, C. (2016). Laminar film condensation along a vertical plate embedded in an anisotropic porous medium with oblique principal axes. *Heat and Mass Transfer*, *52*(10), 2119-2128.

Bejan, A. (1984). Convection Heat Transfer. *John Wiley & Sons*, 146-150.

Degan, G., Akowanou, C. and Awanou, C. N. (2007). Transient natural convection of non-Newtonian fluids about a vertical surface embedded in an anisotropic porous medium.*Int. J. Heat Mass Transfer*, *50*, 4629-4639.

Liu, C. Y., Ismail, K. A. R. and Ebinuma, C. D. (1984). Film condensation with lateral mass flux about a body of arbitrary shape in a porous medium. *Int. Comm. Heat and Mass Transfer, 11*, 377-384.

Méndez, F. and Treviño, C. (1997). Film condensation induced by a natural convective flow: steady-state analysis.*Int. J. Heat Mass Transfer*, *40*, 1279-1289.

Nusselt, W. (1916). The condensation of steam on cooled surfaces (Traduit par D. Fullarton). *Zeitschrift des Vereines Deutscher Ingenieure, 60*(27), 541-575.

Sanya, A., Akowanou, C., Sanya, E. and Degan, G. (2014). Liquid film condensation along a vertical surface in a thin porous medium with large anisotropic permeability. *Springer Plus*, *3*, 659.

Sanya, S.A.O., Akowanou, C., Fannou, J. L., Moussa, A. D. and Sanya, E. A. (2021). Transient film condensation on a vertical surface in a thin porous medium with large anisotropic permeability. *International Journal of current research, 13*(10), 19332-19340.

**How to cite this article:** S.A.O. Sanya, G. Chidikofan, M.F.O. Sanya, S. Osseni and C. Akowanou (2024). Transient Laminar Film Condensation on an Isothermal Vertical Surface in an Anisotropic Permeability Porous Medium using the Complementary Error Function for the Temperature Profile. *International Journal on Emerging Technologies, 15*(1): 09–15.